

A Comparative Investigation on Outdoor and Laboratory Test of the Degradation Rates for Different Types of Photovoltaic Modules with Different Exposure Periods

Saddam Al-Otab¹, Salman Ajib^{2,*} and Wolfgang Langner³

¹The University of Jordan, Department of Mechanical Engineering, Renewable Energy Program; Amman 11942, Jordan

²Hochschule Ostwestfalen-Lippe, Department of Environmental Engineering and Applied Informatics, Section of Renewable Energies and Decentralized Energy Supplying; An der Wilhelmshöhe 44, D 37671 Höxter, Germany

³Hochschule Ostwestfalen-Lippe, Department of Environmental Engineering and Applied Informatics, Section of Renewable Energies and Decentralized Energy Supplying; An der Wilhelmshöhe 44, D 37671 Höxter, Germany

Abstract: Understanding field failure and degradation modes in solar photovoltaic (PV) modules is very important for various reasons especially for this widely used technology. The University of Applied Sciences Ostwestfalen-Lippe in Höxter owns photovoltaic-modules of different cell types, sizes and operation periods in German weather conditions. This paper presents a detailed degradation investigation and performance parameters analysis for chosen samples of polycrystalline, monocrystalline and thin film modules in the laboratory and outdoor test conditions after 10 years of exposure. The obtained measurements were standardized and then compared with the warranted values of the manufacturer's datasheets for each module type. The real outdoor measurements for the larger units show that the maximum power Pmax after 10 years of exposure for polycrystalline, monocrystalline and amorphous thin film modules had declined by: 8.47%, 37.67%, and 19.05% respectively, which translates to an annual linear degradation rates of 0.652%, 3.67%, and 1.465% for each type respectively. While the maximum power output of the smaller units had declined by 19.05%, 19.36%, and 21.75% for polycrystalline, monocrystalline and amorphous thin film modules respectively, which also translated to annual linear degradation rates of 1.48%, 1.67%, and 0.6% for each type respectively. On the other hand, the laboratory tests for these modules show that there is a clear variation with the obtained outdoor results, where the Pmax for the same larger units had declined by 39.6%, 57.4%, and 82.5% for polycrystalline, monocrystalline and thin film modules respectively. While the Pmax output of smaller units had declined by 51.2%, 39.38%, and 9.39% for polycrystalline, monocrystalline and thin film modules respectively. The comparison of the efficiency and fill factor parameters for the obtained results with the manufacturer's data shows that the outdoor measurements introduce close results than the laboratory results. The discoloration of the encapsulant is the most frequently occurring visually observable defects on the modules.

Keywords: PV modules, Outdoor tests, Laboratory tests, Degradation rates, Monocrystalline PV modules, Polycrystalline PV modules, Thin-film PV modules, Fill Factor.

1. INTRODUCTION

In General, Solar photovoltaic technology considered to be one of the common renewable energy technologies around the world, considered by phenomenal and sustained growth for well over a decade, with cumulative global installed capacity reaching 402 GW by end of 2017 [1]. In 2017, the annual installed capacity was almost 100 GW, which establishes almost a quarter of this cumulative capacity [1]. The position of the technology takes on added significance as the world pursues low carbon development ways through initiatives such as the

sustainable energy for all and the satisfying of the sustainable development goals [2].

Photovoltaic durability and reliability questions have attracted increased interest in recent years because of their technological and economic significance. Reliability is the ability to perform a required function for a given time interval and is often measured in terms of failure rate or as a probability for failure [3]. In contrast, durability relates to the time interval a system is performing its desired task and is in PV commonly measured as the degradation rate, the slow gradual loss of performance.

All EU countries have adopted national renewable energy action plans showing what actions they intend to take to meet their renewables targets. These plans include sectorial targets for electricity, heating and

*Address correspondence to this author at the Hochschule Ostwestfalen-Lippe, Department of Environmental Engineering and Applied Informatics, Section of Renewable Energies and Decentralized Energy Supplying; An der Wilhelmshöhe 44, D 37671 Höxter, Germany; Tel: +49 5271 687 -7877; E-mail: salman.ajib@hs-owl.de

cooling, and transport; planned policy measures; the different mix of renewables technologies they expect to employ; and the planned use of cooperation mechanisms [4].

Renewable energy in Germany is mainly based on wind, solar and biomass. In addition, Germany had the world's largest photovoltaic installed capacity until 2014, and as of 2016, it is third with 40 GW. It is also the world's third country by installed wind power capacity, at 50 GW, and second for offshore wind with over 4 GW [5].

Understanding and minimizing technology risks associated with PV investments support the need for ongoing studies on operational performance and reliability of field deployed systems. Certainly, such data is important to various actors along the solar PV value-chain; from institutions involved in basic research to those that are engaged in project development, system integration, field deployment and operations and maintenance (O&M) services [6].

Globally, investments in solar PV have been rising, increasing from \$11bn in 2004 to \$160bn in 2017, with the cumulative annual growth rate of 23% [7]. Along with this, is the increased interest in monitoring, acquisition, and interpretation of operational data on fielded modules and from testbeds managed by many National Laboratories and other Research Institutes. For example, Osterwald *et al.* had conducted in 2005 a review in which they identified only 10 studies that had researched the subject of photovoltaic performance degradation [8]. By 2016 (after a decade), Jordan *et al.* reviewed almost 200 studies reporting more than 11,000 degradation rates from 40 countries [9]. These meta-studies [10] have also highlighted the geographical imbalance of available data and made a case for an expanded representation of high-quality data on-field performance and degradation of solar photovoltaic modules.

Electricity generated using photovoltaic technology can only be economical if the PV modules operate reliably for 25–30 years under field conditions. In order to ensure such levels of reliability PV module undergo stringent qualification tests developed as per international standards by International Electro-technical Commission. These tests provide excellent information regarding module design, material and process flaws which can lead to early failure. Even the well-qualified modules are found to fail or degrade more than their expected levels when exposed to the

outdoor conditions, indicating that these tests are not adequately addressing the real outdoor conditions and are not sufficient to estimate the module lifetime [11]. Studies on PV degradation often investigate the degradation modes, mechanisms, and degradation rates. The reported degradation modes include cell cracks, hot spots, glass soiling, ethylene vinyl acetate (EVA) browning, delamination, coating oxidation, etc., for crystalline silicon PV modules operated over 20 years in Italy. These degradation models were also observed in PV modules of other technologies and exposed to various climates [12]. Jordan *et al.* concluded that hot spot was the most important degradation mode for crystalline modules installed in the last 10 years while the glass breakage and absorber corrosion dominated the degradation models for thin-film PV technologies. It was also concluded that PV modules exposed to hot and humid climates show considerably higher degradations modes than those in desert and moderate climates. These degradation modes decrease the light approaching the semiconductor junction and worsen the internal electrical properties of PV modules leading to the loss of power production [13].

This work is focused on the degradation and performance parameters analysis for Polycrystalline, Monocrystalline, and Amorphous Thin film solar modules of different capacities and with 10 years of exposure in basis of outdoor and laboratory test conditions and introduce an integrated comparison of different performance parameters for each type with the manufacturer database which we considered as a reference in our evaluation of the obtained results.

2. MATERIAL AND METHOD OVERVIEW

The University of Applied Sciences Ostwestfalen-Lippe in Höxter owns photovoltaic-modules of different cell types, sizes and operation periods in its competent Departments. Figure 1 shows a sample these panels which operated under German climatic conditions at the Technical University of Ilmenau for a period of 10 years. The modules numbered from 1 to 7, modules labeled by numbers 1, 3 and 6 are the larger capacity modules of polycrystalline, monocrystalline and amorphous thin film modules respectively. The other smaller ones are 2, 4, 5, and 7. Modules number 4 and 5 are identical. Modules labeled by number 8 also represents two new identical monocrystalline modules which considered in the measurements for purposes of further analysis and comparison with the results of the aged module of the same technology type (module number 3).



Figure1: Samples of different types PV modules.

The short-circuit current (I_{sc}), open-circuit voltage (V_{oc}), fill factor (FF) and other characteristics of the modules are presented in Table 1. The data shown in this table (which serve as references values) are manufacturer-supplied values. They are obtained from module nameplates and will be used as a reference in our analysis of performance and degradation ratios.

2.1. Instrumentation and Measurements

The measurements of the study were conducted in the laboratory and real outdoor conditions. The measured environmental and electrical parameters of each module were used in further analysis and calculations in order to obtain more reliable experimental results.

2.1.1. Laboratory Measurements Overview [14]

To simulate sunlight, halogen lamps shown in Figure 2 which with a power of 1000 Watt per unit lamp were used in the laboratory. The power supply of the halogen lamps was ensured by a power supply transformer. This enables it possible to produce irradiation intensities of up to 1000 W/m². For the experiment, the halogen lamps were set up at predetermined distances by markings on the floor as illustrated in Figure 3. Markings for a total of 250 cm

are placed up to a distance of 25 cm. The module is set to the distance line of 0 cm and the halogen at a distance of initially 250 cm to the module set up. The halogen light is plugged into a power outlet and can then be operated by a rotary switch. The irradiated photovoltaic module is placed parallel to the halogen lights. The respective module is connected to the resistors, voltmeter, and amperemeter.

The measurements of the electrical and environmental parameters of the photovoltaic modules can then be obtained. By reducing the distance between the halogen lamps and the photovoltaic modules, different irradiance levels of 450 W/m² up to 1000 W/m² were obtained. In order to be able to measure the irradiance, two devices were used. The first one is an electronic measuring device, which was attached to the monocrystalline silicon laboratory cells and absorbs the radiation intensity with the unit kW/m². This must then be multiplied by the factor 1000 to obtain the unit W/m² for further calculations. The second one, a non-electronic measuring device which measures the irradiation in the unit J/ (cm² × min) is present. The result must then also be converted to W/m² (multiplication by 10,000 and divided by 60) and multiplied by a correction factor of 1.3 due to the age of the instrument. Furthermore, two multimeters are used to measure the current and voltage of the photovoltaic modules. A multimeter is used as a voltmeter and one as an ammeter. Resistors are used to generate different current and voltage levels. A 10 Ω shift resistance and two 22 Ω fixed resistors are used. By series and parallel connection of the resistors 5 Ω, 10 Ω, 22Ω, 32 Ω, 54 Ω can be generated for the measurement. To measure the temperature of the modules and to determine the distribution of heat on the modules through the halogen lamps, a Flir thermography camera was used.

Table 1: PV Modules Manufacturer's Data

No.	Solar Module	Voc	Isc	Vmp	Imp	Pmp	$\alpha_V(\%/C)$	$\alpha_I(\%/c)$	FF%	$\eta T\%$
8	ET-85Wp Monocrystalline 120.5 x 54.5 cm	22.43	4.91	18.64	4.56	85	0.397	0.06	0.77	12.9
7	PX-85Wp Polycrystalline 120 x 54 cm	21.5	5.5	17.4	4.85	85	0.325	0.037	0.719	13.1
3	AS-80Wp Monocrystalline 120 x 52.6 cm	21.5	4.95	17.3	4.6	80	0.332	0.04	0.752	12.67
6	ASI-32Wp amorphous Si thin-film 100.5 x 60.5 cm	22.8	2.5	16.8	1.92	32	0.33	0.08	0.5614	5.26
2	SM-10Wp Polycrystalline 43.8 x 23.8 cm	20.8	0.64	17.2	0.58	10	0.325	0.037	0.7512	9.6
4&5	STP-5Wp Monocrystalline 21.6 x 30.6 cm	20.37	0.19	10.7	0.16	5	0.393	0.055	0.708	7.56
7	ASI-5WP amorphous Si thin-film 29.3 x 33.0 cm	22.8	0.4	16.8	0.31	5.2	0.397	0.06	0.5702	5.4

For the measurements, the module is placed on the dimension line of 0 cm and the Halogen lamp firstly on 250 cm distance. The halogen light is plugged into a power socket and operated by a rotary switch. In parallel with all measurements, the irradiance is always controlled. Initially, the multimeter is set so that each short-circuits current and open circuit voltage can be measured. Subsequently, the irradiance is also recorded and notated. After this data has been recorded, the halogen lights are placed at 225 cm to the module and the measurements for the new distance are also noted.



Figure 2: Halogen lamps with a power of 1000W per unite lamp.

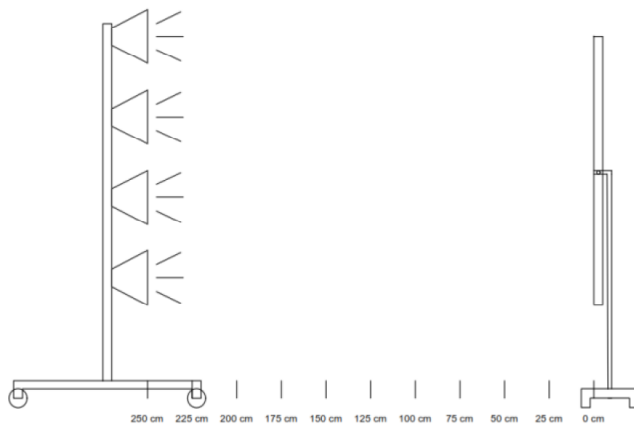


Figure 3: Distance intervals between halogen lamps and PV modules.

This process is repeated in 25 cm decrement until the halogen lights are 100 cm away from the photovoltaic module. This is the last measurement distance recorded. This process is repeated with all modules. In addition, to measure the temperature, the photovoltaic module and halogen lights are again positioned at a distance of 250 cm. However, before the halogen lamps are switched on, the temperature of the module is detected. After switching on the irradiation, the temperature of the module is measured at intervals of 30 s, 60 s, 90 s, 2 min, 3 min, 4 min, 5

min, and 10 min. As soon as the module has reached room temperature again (through cooling), the measurement is carried out again, this time with 175 cm distance between the photovoltaic module and halogen lamps; then the process is carried out again with a distance of 100 cm. The entire process is done with each module. For now, the voltage and current levels are measured by monitoring and logging the temperature. As with the previous measurements, the photovoltaic module is positioned on the 0 cm dimension line and the halogen spotlights at a distance of 250 cm. The measurements are carried out with different irradiances. Figure 4 shows the irradiance variation with the distance between the halogen lamps and modules. This is the basis for the other charts and tables. The further the halogen lamps are removed from the photovoltaic module, the weaker the irradiance obtained.

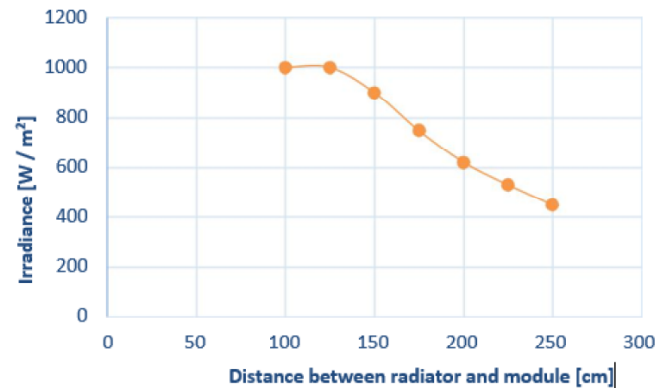


Figure 4: irradiation variation with the distance.

Irradiance Variation Effect

The output power of the PV module strongly depends on the solar irradiation falling on it. The power output of a module increases linearly with the increase in the incident solar radiation. With the increase in the incident solar radiation, a greater number of photons will be available to move the electrons from balance band to conduction band resulting into a production of more current as investigated on this work. Figure 5 to Figure 8 illustrate the relationship between irradiance and short-circuit current (Isc) and open circuit voltage (Voc) with the increment of the temperature by the time. The Figures 5 and 6 shows that by increasing the irradiance which emitted by halogen lamps the values of short-circuit currents are increased and the increasing of the temperature of the solar modules by the time caused a slightly increment on the short-circuit current in the saturation level where the value of the irradiance is constant (1000W/m2). In contrast,

Figures 7 and 8 shows that the open-circuit voltages are increased for a specific period of time, by reaching to significant values of temperature the open circuit voltage values considerably decreased and consequently caused the drop on the output power in various behavior for each type and size of PV modules.

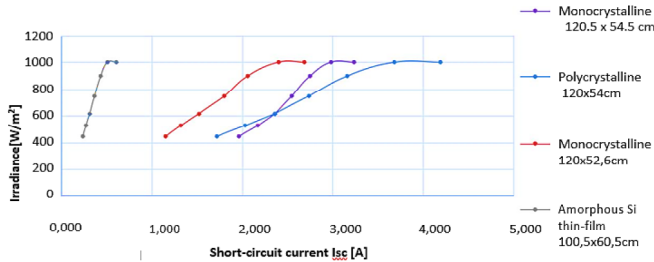


Figure 5: Short-circuit current variation with the irradiance (Larger units).

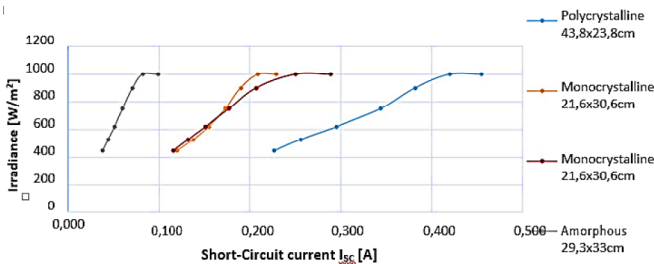


Figure 6: Open circuit variation with the irradiance (Smaller Units).

Temperature Variation Behavior

The output power of a PV module depends on the temperature at which the solar cells operate. It is important to note that module temperature is always higher than the ambient temperature. The higher temperature of the module is due to the use of glass cover which traps the infrared radiation. The increase in temperature causes the reduction of bandgap of the PV cells in the module. This leads to an increase in I_{sc} but decreases in V_{oc}. The decrease in V_{oc} is more prominent than the increase in the I_{sc}. In our study, the

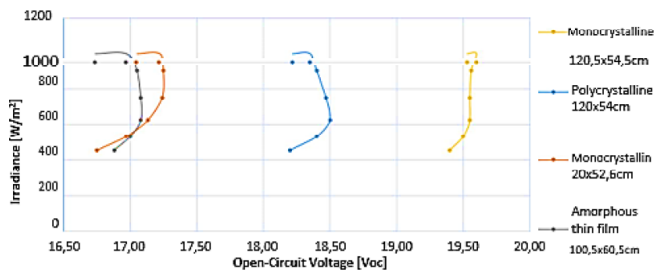


Figure 7: Open-circuit Voltage variation with the irradiance (Larger units).

increment of the temperature values was noted and recorded as shown in Figure 9 for larger modules after 10 minutes of imitation of the irradiance 1000 W/m², the initial measured temperature is around 22 ° C for the larger modules. The maximum and minimum temperature values were obtained after ten minutes of exposure for larger modules was around 88 ° C and 74.2 ° C for amorphous silicon thin-film cell and monocrystalline solar cell respectively.

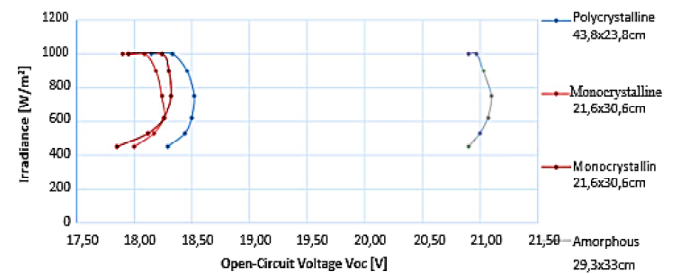


Figure 8: Open-circuit Voltage variation with the irradiance (Smaller units).

were obtained after ten minutes of exposure were around 76.5 ° C and 58 ° C for amorphous silicon thin-film cell and monocrystalline solar cell.

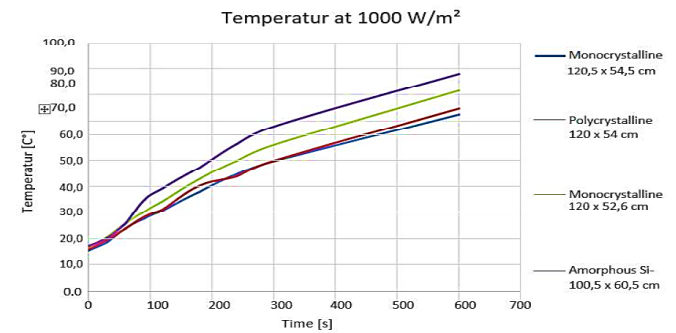


Figure 9: Temperature variation with the time (Larger units).

I-V Curves Characteristics

The current-voltage curves (I-V curves) measurements are commonly used to analyze the electrical performance of solar cells. These measurements provide a most effective way to determine fundamental performance parameters. The results show that with the decreasing of the irradiance the maximum power P_{MPP} decreased. The power is composed of the product of voltage and current, and the maximum power is characterized by the maximum possible product of voltage and current for each characteristic. In this laboratory test, the I-V curves were recorded with different values of irradiance (450, 620, 750, and 1000 W/m²) (Figures 10, 11 and 12).

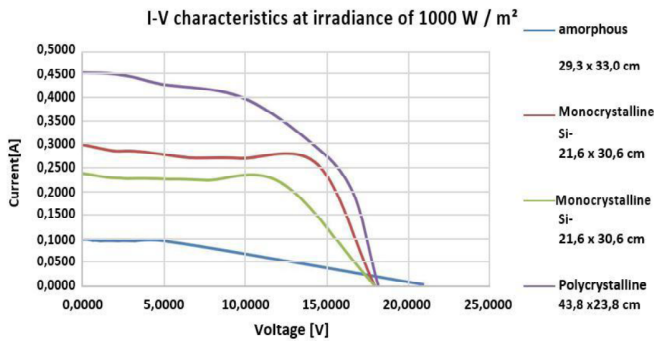


Figure 10: I-V characteristics at irradiance of 1000 W / m² in Lab (Smaller units).

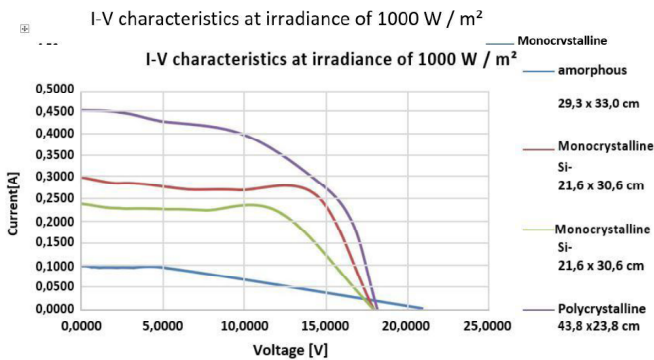


Figure 11: I-V characteristics at irradiance of 1000 W / m² in Lab (Larger units).

The uniformity of the intensity of the halogen lamps irradiance was investigated to be barely varied along of the tested PV module surfaces, this affected a little bit on the accuracy of the obtained laboratory measurements. This is one of the reasons for the clear variation of the laboratory results when comparing with the real outdoor measurements.

The I-V curves characteristics of the small photovoltaic modules clearly show that with lower irradiance values, the current and voltage levels are also decreased. Thus, at lower irradiance, the performance of the module will be weaker. In general, for larger and smaller units the effect of irradiance decreasing appeared to cause a deformation in the I-V curve characteristics. In order, decreasing the performance and efficiency of the modules. The characteristics of the small PV modules also clearly show that the amorphous thin-film cell has a significantly lower current flow, despite the same radiation and a larger area of the module. The polycrystalline silicon cell provides a larger current than the other cells, but this is also because this module has a larger area.

For the two identical monocrystalline modules of 5 Wp, the obtained curves show very small variation although the two modules were operated and testes at the same climate and testing conditions. While the comparison of the new monocrystalline module and the other of the 10 years of exposure shows that the drop of the efficiency for the newest one had reached to 58.9% and about 57.46% for the older one. This result is not expected and may be referred to the difference of the manufacturer for each module and the effect of the temperature on them. In addition, the uncovered area of the newest module is clearly higher than the other one of 10 years exposure period. In the same manner, the drop on the fill factor had obtained to be 40.3% and 40.6% for the newest and older units. This can be translated to linear annual degradation rates of 3.1% and 3.12% for the newest and older units respectively. In general, the degradation behavior for the newest module cannot be predicted precisely before it the exposure for different real climatic and operating conditions.

The laboratory measurements here have been used in calculations to obtain further performance parameters which will be employed in the assisting the comparison with the field and manufacturer's datasheets values.

2.1.2. Outdoor Measurements Overview

Our outdoor Measurements of electrical characteristics of the modules was undertaken with the same measurement tools used in the laboratory state. The performance and degradation analysis achieved in accordance to obtained outdoor measurements and in nearly the same conditions in order to be compared with the laboratory test results. The solar modules outdoor measurements have been achieved after deciding a suitable location on the University of Applied Sciences Ostwestfalen-Lippe campus in Höxter. Figure 13 shows the exact chosen positions to confirm the needed measurements by the red circles. The location weather parameters and sun path diagram are shown on the Table 2 and Figure 14 respectively [15].

Measurements were conducted between 10 am and 2 pm local time (within the solar window) in order to reduce the impact of angle-of-incidence effects. In addition, the value of the tilt angle altered between 35 to 50 degree to simulate the standard test conditions (AM=1) as shown in Figure 15.

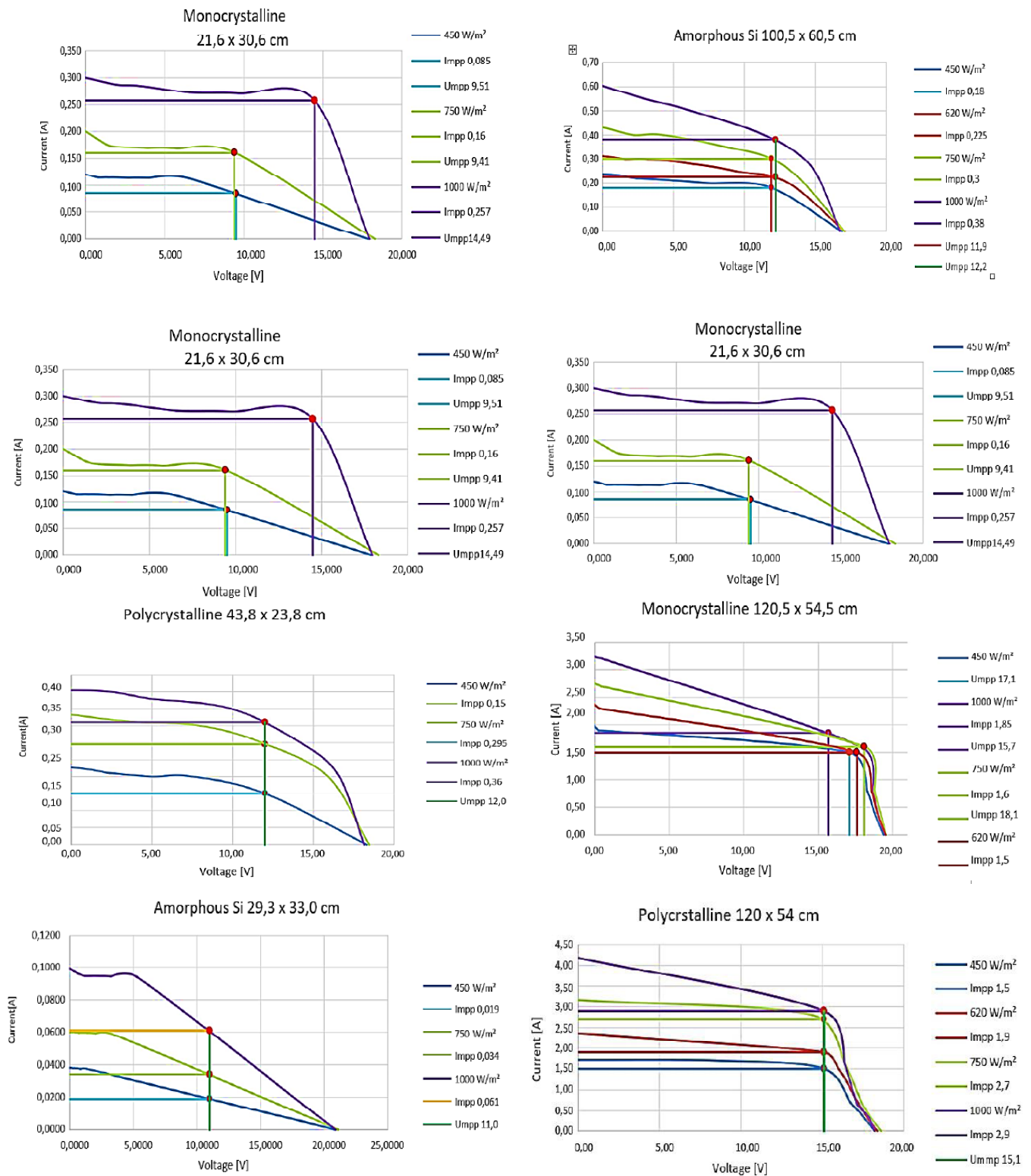


Figure 12: I-V Curves for all module types with the variation of the radiation's values.

Several measurements of current and voltage levels with different irradiance levels were taken. The measurements are summarized with the best measurement results, which will be used to evaluate and illustrate the performance and the degradation

rates calculations for further analysis.

I-V Curves Characteristics

As obtained from the laboratory measurements, the I-V curves for smaller and larger PV modules unite

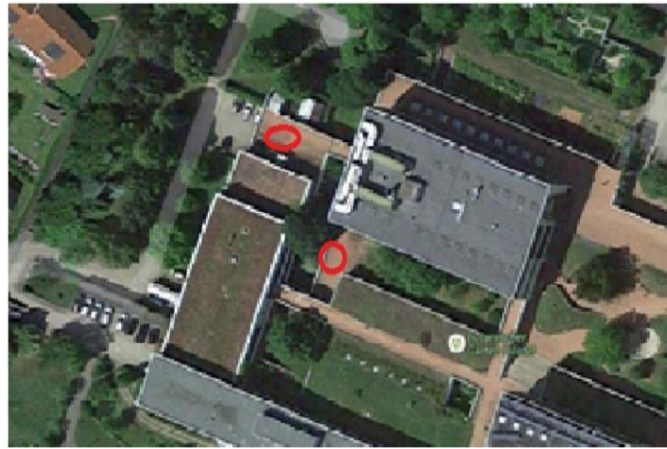


Figure13: Measurements locations at the university campus.

Table 2: Definition of a Geographical Site Weather Parameters

Situation	Latitude 51.8°N	Longitude 9.4°E												
Time defined as	Legal Time Time zone UT+1	Altitude 146 m												
Monthly Meteo Values	Source NASA-SSE satellite data, 1983-2005													
	Jan.	Feb.	Mar.	Apr.	May	June	July	Aug.	Sep.	Oct.	Nov.	Dec.	Year	
Hor. global	25.1	42.6	74.4	109.5	141.7	142.2	144.8	128.3	83.7	50.5	26.4	19.5	988.7	kWh/m ² .mth
Hor. diffuse	16.7	25.2	45.3	62.1	77.8	81.3	80.6	69.4	47.1	29.8	17.7	13.6	566.6	kWh/m ² .mth
Extraterrestrial	70.6	108.7	187.4	258.4	328.7	346.0	345.4	294.5	212.6	144.2	81.4	57.7	2435.7	kWh/m ² .mth
Clearness Index	0.355	0.392	0.397	0.424	0.431	0.411	0.419	0.436	0.394	0.350	0.324	0.338	0.406	
Amb. temper.	0.7	1.2	4.1	8.0	13.1	15.8	18.3	18.5	14.1	9.9	4.5	1.6	9.1	°C

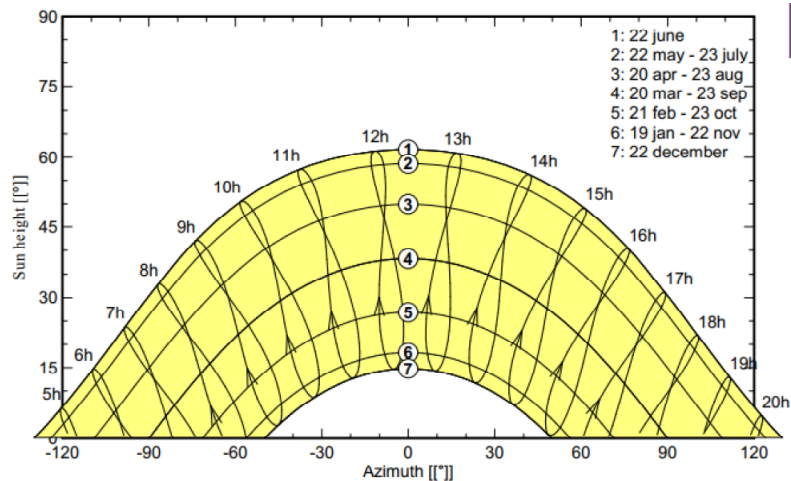


Figure 14: Solar paths at Höxter, (Lat. 51.8°N, long. 9.4°E, alt. 146 m).

under outdoor test conditions were illustrated in Figure 16 and Figure 17 respectively. The measured values have been obtained under different temperature and radiation values. This enables translation of acquired data to Standard Test Conditions (STC) or

other desired reference conditions. Standard test conditions for solar PV modules for terrestrial applications are: irradiance – 1000 W/m², module temperature – 25 °C and air mass – 1.5.



Figure 15: PV Modules installation for outdoor measurements.

These standard parameters must be achieved in order to compare and use our results for further analysis for degradation and other performance parameters. The standardization of the measured values was demonstrated in the next section.

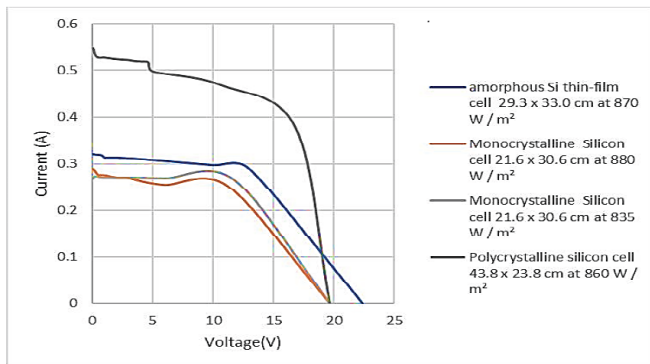


Figure 16: I-V Curve Characteristics under outdoor conditions (Smaller units).

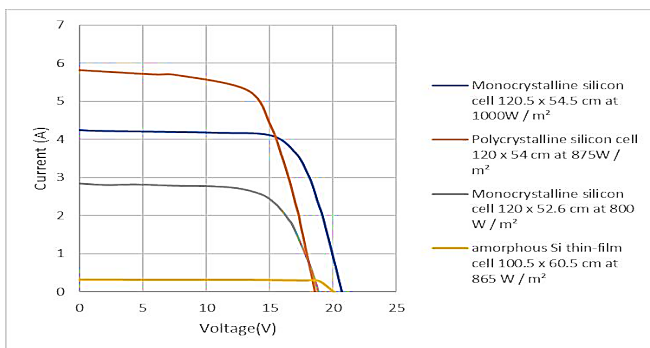


Figure 17: I-V Curve Characteristics under outdoor conditions (Larger units).

2.2. Degradation Rate Analysis

This work required a standardization method for measurements of these characteristics in real

conditions. Standardization is bringing back the measurements in real conditions to the corresponding values in standard test conditions (STC). Current-voltage (I-V) measurements obtained under field conditions were translated to STC conditions by applying Eqs. 1-5 [16].

$$V_{oc} = V_{ocSTC} \cdot \ln(E) / \ln(E_{1000}) \cdot (1 + \alpha_v(\vartheta - \vartheta_{25})) \quad (1)$$

Where V_{oc} and V_{ocSTC} are respectively, the open-circuit voltage at measured and at STC conditions, and:

- E = irradiance in W/m^2
- $E_{1000s} = 1000 W/m^2$
- α_v = Voltage Temperature Coefficient in $\%/C^\circ$.
- ϑ = Measured Temperature.
- $\vartheta_{25} = 25 C^\circ$.

By the same manner V_{mp} can be calculated by:

$$V_{mp} = V_{mpSTC} \cdot \ln(E) / \ln(E_{1000}) \cdot (1 + \alpha_v(\vartheta - \vartheta_{25})) \quad (2)$$

The short-circuit current at STC, I_{scSTC} , is calculated from Eq. (3):

$$I_{sc} = I_{scSTC} \cdot (E) / (E_{1000}) \cdot (1 + \alpha_i(\vartheta - \vartheta_{25})) \quad (3)$$

By the same manner I_{mp} can be calculated by:

$$I_{mp} = I_{mpSTC} \cdot (E) / (E_{1000}) \cdot (1 + \alpha_i(\vartheta - \vartheta_{25})) \quad (4)$$

Where,

- α_i Current Temperature Coefficient in $\%/C^\circ$.

The maximum power at STC, P_{STC} , is computed from I_{scSTC} , V_{ocSTC} and the measured fill factor (FF) using Eq. 5:

$$P_{STC} = FF * I_{scSTC} * V_{ocSTC} \quad (5)$$

The average annual degradation rate of the module's maximum power (DR_{Pmax}) is determined according to Eq. 6 [18]:

$$DR_{Pmax}\% = (P_{max,Manu} - P_{maxSTC}) / (y * P_{max,Manu}) * 100 \quad (6)$$

Where,

- $P_{max,Manu}$ is the reference maximum power data (Table 1),
- y is field exposure duration (in year), and
- P_{STC} is from Eq. 5.

The degradation rates of the explanatory variables (i.e. V_{oc} , I_{sc} and FF) are assessed in an analogous manner [18].

The drop of the maximum power ΔP_{max} of each module can be calculated by Eq. 7:

$$\Delta P_{max}\% = (P_{mp,Manu} - P_{mp,STC} / P_{mp,Manu}) * 100 \tag{7}$$

$\eta T\%$, $\Delta FF\%$ are assessed in an analogous manner.

Finally, the efficiency of each module can be calculated by Eq. 8:

$$\eta T\% = P_{mp} / (E_{1000} * A) \tag{8}$$

Where, A is the Area of the module.

3. RESULTS AND DISCUSSION

This section presents the main results founded on measured data and computations undertaken with the set of equations presented in Section 2. Thus the standardized values of short-circuit current ($I_{sc,STC}$), the open-circuit voltage ($V_{oc,STC}$) and the maximum output power (P_{max}) which obtained in outdoor and laboratory measurements are compared with reference values corresponding to the first putting service of the module or the manufacturer's data as in our case. Visually observable defects that were documented in the study are presented next. The effort is made to explore the relationship between observed defects and explanatory variables for module power losses (*i.e.* I_{sc} , V_{oc} , η , and FF).

3.1. Outdoor and Laboratory Results Comparisons

Tables 3 and 4 summarized the main results regarding the performance parameters for all modules considered in the study after 10 years of exposure. In general, and although the measurements were made in the same test conditions, there is a clear difference between the values obtained in the laboratory experiments relative to the results of the outdoor measurements, and this may be referred to the high temperature in laboratory experiments even after standardization (Comparing the temperatures generated by the halogen lamps in the laboratory and the temperatures that the photovoltaic modules have in outdoor operation, one can note a big difference as discussed before.) This led to change of the properties of different modules cell. Moreover, in outdoor measurements and due to the low outside temperature, the modules are additionally cooled, and it does not reach to high temperatures. In contrast, the PV modules reach in Laboratory up to 88 ° C. From Figurers 18 the photos were taken with the Flir thermographic camera which show clearly that the heat distribution of the radiator is not evenly distributed, and since there is no possibility of cooling and they are thus steadily heated. However, all values standardized as we discussed before in the equations of section 2. in addition, the possibility of some random errors and the accuracy consideration of the measurement devices. Despite all the above, and by comparing the results of performance of all modules with each other, whether

Table 3: Outdoor Measurements (Main Results)

Solar Module	FF _{STC} %	$\eta T\%$	DR _{mp} %	DR _{voc} %	DR _{isc} %	DR _{FF} %	FF _{manu} %	ΔP_{max}	$\Delta \eta T\%$	$\Delta FF\%$
ET-85Wp Monocrystalline 120.5 x 54.5 cm	70.67	10.28	20.58	-1.78	14.79	0.63	0.77	0.21	20.32	8.22
PX-85Wp Polycrystalline 120 x 54 cm	60.88	12.00	0.65	0.81	-1.60	1.18	0.72	0.08	8.37	15.32
AS-80Wp Monocrystalline 120 x 52.6 cm	68.73	7.90	3.67	0.33	2.21	0.66	0.75	0.38	37.65	8.60
ASI-32Wp amorphous Si thin-film 100.5 x 60.5 cm	51.64	4.26	1.47	0.65	0.30	0.62	0.56	0.19	19.01	8.01
SM-10Wp Polycrystalline 43.8 x 23.8 cm	58.85	7.74	1.49	-0.14	-0.08	1.67	0.75	0.19	19.42	21.66
STP-5Wp Monocrystalline 21.6 x 30.6 cm	49.52	5.30	2.31	-0.50	-5.51	2.31	0.71	0.30	29.93	30.06
STP-5Wp Monocrystalline 21.6 x 30.6 cm	59.11	5.92	1.67	0.20	0.29	1.27	0.71	0.22	21.71	16.51
ASI-5WP amorphous Si thin-film 29.3 x 33.0 cm	52.44	4.77	0.60	-0.45	0.69	0.62	0.57	0.11	11.74	8.04

Table 4: Laboratory Measurements (Main Results)

Solar Module	FF _{STC} %	ηT%	DR _{mp} %	Drvoc%	DR _{i,sc}	DR _{FF} %	FF _{manu} %	ΔP _{max}	ηT%	ΔFF%
ET-85Wp Monocrystalline 120.5 x 54.5 cm /1000,72.5	45.90	5.30	59.06	-7.31	35.84	3.11	0.77	0.59	58.92	40.39
PX-85Wp Polycrystalline 120 x 54 cm /74.8	57.42	7.92	3.05	-0.08	1.94	1.55	0.72	0.40	39.57	20.13
AS-80Wp Monocrystalline 120 x 52.6 cm/81.6	44.64	5.39	5.19	-0.91	2.77	3.13	0.75	0.57	57.47	40.64
ASI-32Wp amorphous Si thin-film100.5 x 60.5 cm/88	46.16	0.92	6.35	0.56	5.93	1.37	0.56	0.83	82.58	17.78
SM-10Wp Polycrystalline 43.8 x 23.8 cm/64	51.74	4.68	3.94	0.01	2.24	2.39	0.75	0.51	51.27	31.12
STP-5Wp Monocrystalline 21.6 x 30.6 cm/58	62.52	4.59	3.03	-0.07	-1.85	0.90	0.71	0.39	39.34	11.70
STP-5Wp Monocrystalline 21.6 x 30.6 cm/76	69.15	6.85	0.72	-0.38	0.89	0.18	0.71	0.09	9.34	2.33
ASI-5WP amorphous Si thin-film 29.3 x 33.0 cm/76.5	32.43	0.85	6.43	-1.17	5.85	3.32	0.57	0.84	84.33	43.13

obtained in the laboratory or in the outdoor measurements for different types of solar modules, the performance results are consistent and have the same indications of the performance and degradation parameters.

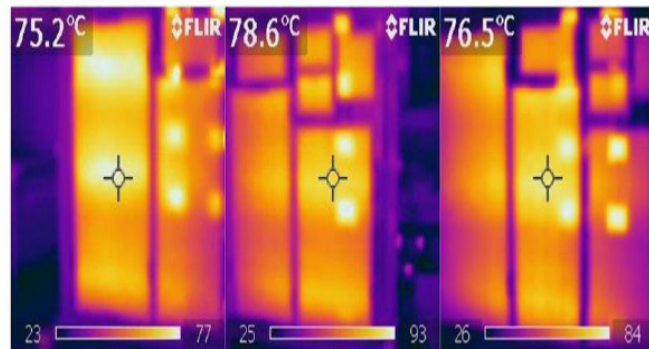


Figure 18: Temperature distribution in laboratory test.

3.2. Performance Characteristics

By applying Eqs. 1–8, with relevant data in Table 1, the obtained results in Table 3 and Table 4 and measured data for outdoor tests, the yields annual decline in P_{max} 0.652%, 3.66%, and 1.455% for Polycrystalline, Monocrystalline, and Amorphous larger units respectively and 1.489%, 2.305%, and 1.673% for Polycrystalline, Monocrystalline, and Amorphous respectively for smaller units. For both smaller and larger units the Monocrystalline units have the larger power degradation, then Amorphous and

Polycrystalline. The modules are therefore performing at 91.6%, 63.4, and 81% of the initial rated power for Polycrystalline, Monocrystalline, and Amorphous larger units respectively after 10 years of exposure period as shown in Figure 19. In addition, the efficiency and FF drop obtained for Polycrystalline, Monocrystalline, and Amorphous were at 8.36%, 37.6%, and 19%, and 15.32%, 8.59%, and 8.011% respectively for larger units as shown in Figure. 20 and Figure 21.

For Laboratory tests, the yields annual decline in P_{max} 3.049%, 5.19%, and 6.35% for Polycrystalline, Monocrystalline, and Amorphous larger units respectively and 3.94%, 3.029%, and 6.43% for

Polycrystalline, Monocrystalline, and Amorphous respectively for smaller units. For both smaller and larger units the Amorphous Si thin film units have the larger power degradation rates.

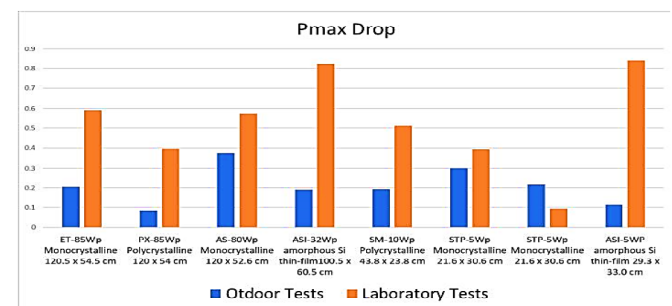


Figure 19: Maximum power drop comparison.

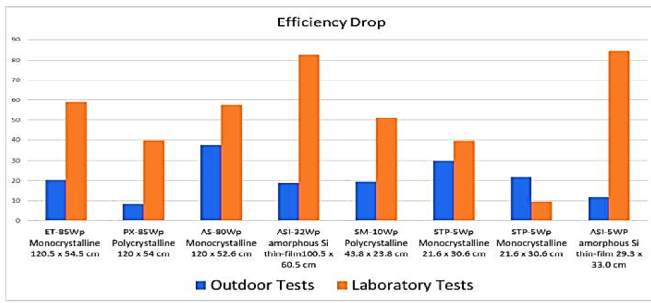


Figure 20: Laboratory and outdoor Efficiency Drop.

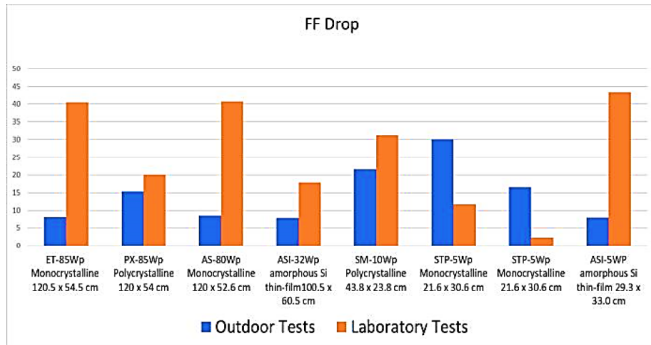


Figure 21: Laboratory and outdoor Fill Factor Drop.

The degradation ratios obtained in this work for P_{max} , FF, V_{oc} , and I_{sc} and for both laboratory and outdoor tests are shown in Figures 22 to 24 respectively. The degradation ratio obtained of P_{max} are attributable mainly to losses in I_{sc} , FF, and V_{oc} , where the maximum power is a function of I_{sc} , FF, and V_{oc} , ($P_{max} = f(I_{sc}, V_{oc}, FF)$). Some values of degradation values of short-circuit currents and open circuit voltages were obtained in the negative direction which indicates the increase of these values as compared with the manufacturer data, even though, the net obtained degradation ratios for all modules are increased by the time.

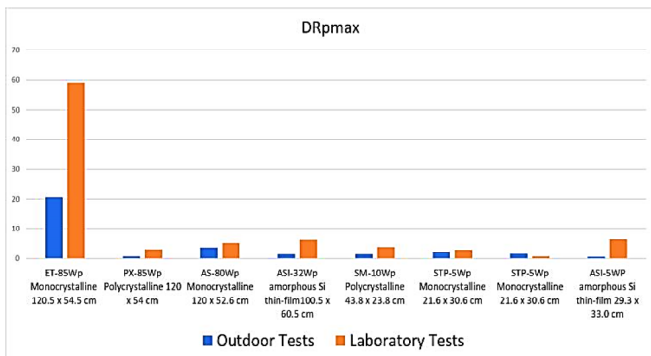


Figure 22: Laboratory degradation ratio of the maximum power.

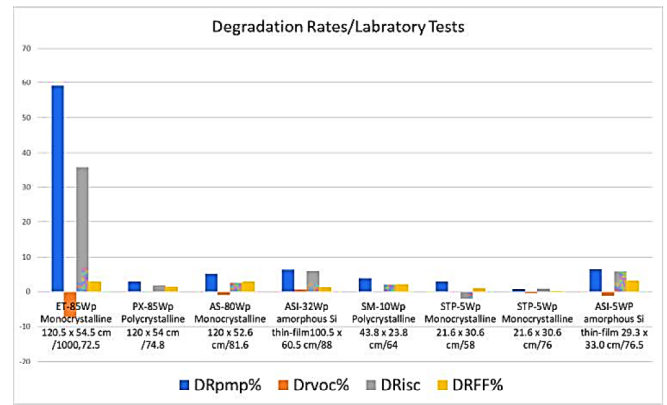


Figure 23: Laboratory degradation ratio of Pmp,Voc,Isc, and FF.

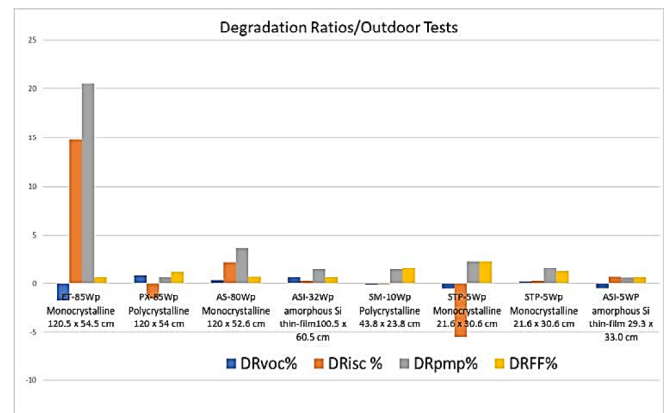


Figure 24: Outdoor degradation ratio of Pmp,Voc,Isc, and FF.

The comparison of the obtained results of the efficiency and fill factor parameters show that the outdoor measurements introduce close results by comparing with the manufacturer data than the obtained results of the laboratory measurements as shown in Figure 25 and Figure 26. But in general, there are a wide deviations between the obtained measurements and the manufacturer's data which represented by the degradation trend of the solar modules. In addition, Laboratory tests show that the best performance was obtained for Monocrystalline technology, then Polycrystalline and Amorphous Si thin film technology. On the other hand, for outdoor tests, the most efficient technology was obtained to be for Polycrystalline solar cell technology then Monocrystalline and Amorphous solar cell technologies. The above results may be interrupted by that the Amorphous thin film technology more compatible and less affected by the temperature rising than the other technologies, in the opposite, the Monocrystalline less compatible and more negatively affected by the temperature rising by comparing with other two technologies.

3.3. Visually Observable Defects

The most commonly reported degradation mode is encapsulant discoloration, which may be aided by the fact that discoloration is also the most noticeable mode by visual inspection [18].

We refer to this as “degradation” rather than “failure,” as discoloration leads typically to lower performance but not necessarily to failure, even when considering soft failure limits such as a typical power warranty. Figure 27 shows the discoloration observed for both Monocrystalline and Amorphous SI thin-film solar modules which have been tested.

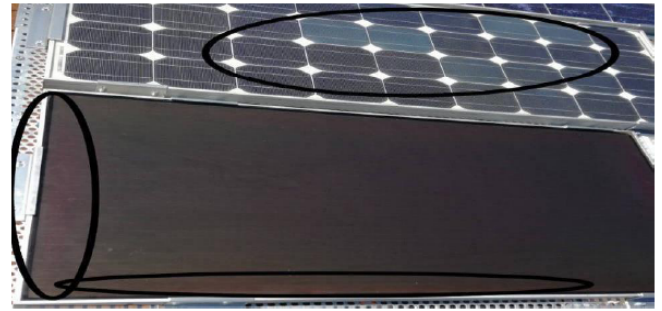


Figure 27: discoloration for Monocrystalline and Amorphous solar modules.

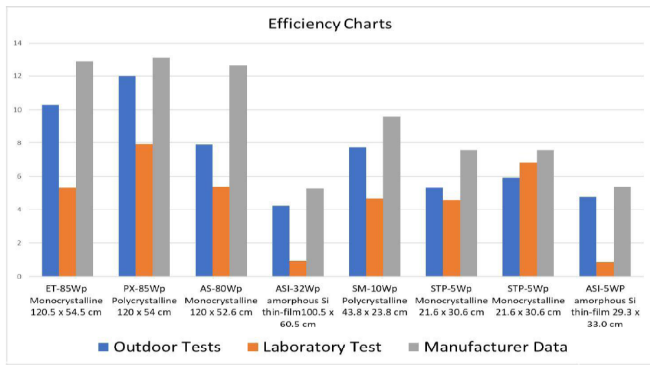


Figure 25: Efficiency Charts Comparison with manufacturer's reference data.

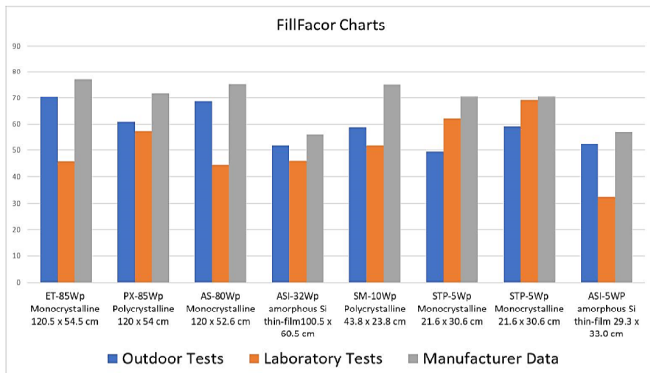


Figure 26: Fill Factor Charts Comparison with manufacturer's reference data.

Table 5: I-V Multimeter Specifications

DC Voltage Measurements			DC Current Measurements		
Range	Resolution	Accuracy	Range	Resolution	Accuracy
400 mV	100 μV	±0,5% v.M. + 2 St.	400 μA	0,1 μA	± 1,0% v.M. + 3 St.
4 V	1 mV		4 mA	1,0 μA	
40 V	10 mV		40 mA	10,0 μA	
400 V	100 mV	± 1,2% v.M. + 2 St.	400 mA	100,0 μA	± 1,5% v.M. + 3 St.
600 V	1 V		4:00 AM	1,0 mA	
		± 1,5% v.M. + 2 St	10 A**	10,0 mA	± 2,5% v.M. + 5 St.

4. UNCERTAINTY AND ERROR ANALYSIS OF THE USED MEASUREMENT DEVICES

Tables 5 to 7 represents some specifications of the used measurement tools used in this work. Moreover, it can be used to introduce an overview of the certainty of the obtained results. As discussed before the measured parameters in this work depend mainly on the environmental parameters like temperature and radiation. So, the obtained results which based either on laboratory or outdoor measurements depend on each other, where we measure the temperature and radiation simultaneously with the measurements of the voltage and current of the PV modules in order to obtain the I-V curve characteristics for each module type.

For certain measurement for certain electrical parameter, the reading continuously changed with the time because the radiation and temperature values can't be controlled especially in outdoor measurements.

CONCLUSIONS

- The study is focused on the degradation and performance analysis for Polycrystalline, Monocrystalline, and Amorphous Thin film solar modules of different capacities and with 10 years

Table 6: Radiation meter Specifications

Model	Spektron 210
Measuring range	0 - 1500 W / m ²
Sensor Type	Monocrystalline Cell (13 mm / 33 mm)
Sensor accuracy	± 5%
Electrical output Approx.	75 mV at 1000 W / m ²
Sensor structure	Laminated in Novaflon and EVA foil

Table 7: Thermometer Specifications

Thermocouple Type	Class	Temperature Range	Deviation Limit
E NiCr-CuNi 1	1	-40 ° C to + 800 ° C	1.5 ° C or 0.0040 x t
	2	-40 ° C to + 900 ° C	2.5 ° C or 0.0075 x t

of exposure in basis of outdoor and laboratory test conditions and introduce an integrated comparison of different performance parameters for each type. Based on the study following conclusions are drawn:

- At 1000 W/m², the temperature had increased by different ratios for each type of PV technology with the time of the exposure for halogen lamps.
- In general, the effect of irradiance decreasing appeared to cause a deformation in the I-V curve characteristics and decreasing the performance and the efficiency, especially for smaller units.
- The characteristics of the small PV modules also clearly show that the amorphous thin-film cell has a significantly lower current flow, despite the same radiation and the larger area of the module.
- Under outdoor test conditions, the annual yield declination of P_{max} of larger units were obtained to be 0.652%, 3.66%, and 1.455% for Polycrystalline, Monocrystalline, and Amorphous respectively, and about 1.489%, 2.305%, and 1.673% for Polycrystalline, Monocrystalline, and Amorphous smaller units respectively.
- For the Laboratory tests, the annual yield declination of P_{max} amounts 3.049%, 5.19%, and 6.35% for Polycrystalline, Monocrystalline,

and Amorphous larger units respectively, and 3.94%, 3.029%, and 6.43% for Polycrystalline, Monocrystalline, and Amorphous respectively for smaller units. For both smaller and larger units the Amorphous Si thin film units have the largest power degradation.

- Some values of degradation values of short-circuit currents and open circuit voltages were obtained with negative values which indicate that there is an increase of these values as compared with the manufacturer data, even though, the obtained degradation ratios for all modules are increased by the time.
- The comparison of the obtained results concerning the efficiency and fill factor parameters shows that the outdoor measurements introduce more closely results when compared with the manufacturer data than the obtained results of the laboratory measurements.
- There are clear deviations between the obtained results and the manufacturer's values which indicates that the degradation trend of the solar modules was not as expected.
- Laboratory tests show that the best performance was obtained for Monocrystalline technology, then Polycrystalline and finally Amorphous Si thin film technology.
- For outdoor tests, the most efficient technology was obtained to be for Polycrystalline solar cell technology then Monocrystalline and finally Amorphous solar cell technologies.
- For outdoor tests, the overall efficiency drop for polycrystalline, monocrystalline and amorphous thin film modules was obtained to be 14.3%, 37.7%, and 22.09% respectively for larger units, and 19%, 19.4%, and 21.7% respectively for smaller units.
- Laboratory tests show that the efficiency drop for polycrystalline, monocrystalline and amorphous thin film modules was obtained to be 39.5%, 57.4%, and 82.57% for larger units, and 51.26%, 39.34%, and 9.33% for smaller modules respectively.
- The Amorphous thin film technology solar modules were found to be more compatible and

less affected by the temperature rising than the other technologies. In contrast, the Monocrystalline solar modules were found to be less compatible with the temperature rising by comparing with other two technologies.

- The comparison of the new monocrystalline module and the other of 10 years of exposure shows that the drop of the efficiency for the newest one had reached to 58.9% and about 57.46% for the older one. This result is not expected and may be referred to the difference of the manufacturer for each module and the effect of the temperature on them. In addition, the uncovered area of the newest module is clearly higher than the other one of 10 years exposure period.
- Finally, discoloration leads typically to lower performance but not necessarily to failure, even when considering soft failure limits such as a typical power warranty.

NOMENCLATURE

Acronyms

STC = Standard Test Conditions

DR = Degradation Ratio

PV = Photovoltaic

FF = Fill Factor

Symbols

T = Temperature [°C]

E = irradiance in W/m²

ϑ = Measured Temperature.

α_i = Current Temperature Coefficient in %/C°.

α_v = Voltage Temperature Coefficient in %/C°

P = Power

V = Voltage

I = Current

Greek Letters

Δ = Drop

η = Efficiency [%]

Subscripts

mpp = Maximum Power Point

Meas = Measured

Max = Maximum

sc = Short-circuit

Manu = Manufacturer

oc = Open Circuit

ACKNOWLEDGEMENT

The authors would like to thank Ostwestfalen – Lippe University of Applied Sciences /Germany and DAAD German Academic Exchange service for their support for the authors.

REFERENCES

- [1] Schmela M, REN21, Renewables 2018 Global Status Report. REN21 Secretariat, Paris. 2018. Looking Back
- [2] Forth: Big Solar Surprises in 2017 & 2018. Solar Power. Europe. Available: <http://www.solarpowereurope.org/newsletter/editorial-look-g-back-forth-big-solar-surprises-in-2017-2018/> (accessed 17 May 2018).
- [3] Sustainable Energy for All (SEforALL), Our Mission - Going further, faster – together. Sustainable Energy for All, 2018. Available: <https://www.seforall.org/ourwork> (accessed 3 May 2018).
- [4] International Electrotechnical Commission 60050 -191, Dependability and quality of service, 1990. renewable energy targets/ European Commission 2020 <https://ec.europa.eu/energy/en/topics/renewable-energy>.
- [5] Renewable energy in Germany, 2018. Available: https://en.wikipedia.org/wiki/Renewable_energy_in_Germany
- [6] Quansah DA, Adaramola MS. Comparative study of performance degradation in poly- and mono-crystalline-Si solar PV modules deployed in different applications. Int J Hydrogen Energy 43(6): 3092-3109. <https://doi.org/10.1016/j.ijhydene.2017.12.156>
- [7] Frankfurt School-UNEP Centre/BNEF. Global Trends in Renewable Energy Investment 2018. Frankfurt School of Finance & Management GmbH, Frankfurt.
- [8] Osterwald C, Adelstein J, del Cueto J, Kroposki B, Trudell D, Moriarty T. Comparison of degradation rates of individual modules held at maximum power. In: 4th IEEE World Conference on Photovoltaic Energy Conversion., 2006, Hawaii. <https://doi.org/10.1109/WCPEC.2006.279914>
- [9] Jordan DC, Kurtz SR, VanSant K, Newmiller Jeff. Compendium of photovoltaic degradation rates. Prog. Photovolt Res Appl 2016; 24(7): 978-989. <https://doi.org/10.1002/ppp.2744>
- [10] Jordan DC, Kurtz SR. Photovoltaic degradation rates-an analytical review .2013. Prog. Photovolt. 12-29. <https://doi.org/10.1002/ppp.1182>
- [11] Vikrant Sharma SS. Chandel, Performance and degradation analysis for long term reliability of solar photovoltaic systems: A review, Renewable Energy 89 (2016) 12e17). <https://doi.org/10.1016/j.renene.2015.11.088>

- [12] Malvoni M, Leggieri A, Maggiotto G, Congedo P, De Giorgi M. Long term performance, losses and efficiency analysis of a 960 kWp photovoltaic system in the Mediterranean climate. *Energy Conversion and Management* 2017; 145: 169-81.
<https://doi.org/10.1016/j.enconman.2017.04.075>
- [13] Jordan DC, Silverman TJ, Wohlgemuth JH, Kurtz SR, VanSant KT. Photovoltaic failure and degradation modes. *Progress Photovoltaic*. April 2017; 25: 18-26.
<https://doi.org/10.1002/ppp.2866>
- [14] Kraft L, Ajib S. Bachelor's degree project (Comparative analysis of Performance characteristics of different types of PV modules at different operation periods based on laboratory and field measurements), 2018.Ostwestfalen – Lippe University of Applied Sciences /Germany.
- [15] PVSyst Software 6.7.0 Version. NASA Database, 2018, Support <http://www.PVsys.com>.
- [16] Volker. Q. 215. Regenerative Energy System, P.213, Text Book, ISBN: 978-3-446-44333-4.
- [17] Kaplanis S, Kaplani E. Energy performance and degradation over 20 years performance of BP c-Si PV modules.2011, *Simul. Model. Pract. Theory* 19, 1201–1211.
<https://doi.org/10.1016/j.simpat.2010.07.009>
- [18] Jordan DC, Kurtz SR. Field experience: Degradation Rates, Lifetimes & Failures. PV Module Reliability Workshop: Lakewood, CO, USA, 2016).

Received on 9-11-2018

Accepted on 5-12-2018

Published on 17-12-2018

DOI: <http://dx.doi.org/10.15377/2409-5818.2018.05.6>© 2018 Al-Otab *et al.*; Avanti Publishers.

This is an open access article licensed under the terms of the Creative Commons Attribution Non-Commercial License (<http://creativecommons.org/licenses/by-nc/3.0/>), which permits unrestricted, non-commercial use, distribution and reproduction in any medium, provided the work is properly cited.